Novelty Journals

ISSN 2394-9651

International Journal of Novel Research in Physics Chemistry & Mathematics
Vol. 10, Issue 1, pp: (38-51), Month: January - April 2023, Available at: www.noveltyjournals.com

EFFECTS OF REYNOLDS NUMBER VARIATION ON HEAT AND MASS TRANSFER FOR MHD FLOW IN A CONCENTRATED PARABOLIC THERMAL SOLAR COLLECTOR

[1]Lucas Khaoya Mukwabi, [2]Dr. Mark Kimathi, [3]Dr. Charles Muli

Department of Mathematics, Machakos University,
P.O Box 136 - 90100, Machakos, Kenya.

DOI: https://doi.org/10.5281/zenodo.7805386

Published Date: 06-April-2023

Abstract: **The paper analyzes the effects of the Reynolds number variation on mixed convective heat and mass transfer over a parabolic surface under a radial magnetic field cutting perpendicular along the fluid flow in presence of a constant radiation heat source. The governing partial differential equations are transformed into a system of ordinary differential equation using non-dimensional numbers. The resulting system of ordinary differential equations together with the boundary equations are then solved numerically by finite difference method and simulated using MATLAB to obtain the profiles of the flow variables. The influence of thermal** Grashof number (Grt), Mass Grashof number (Grc), and Magnetic Parameter (M) **on the flow velocity, temperature and concentration profiles are displayed in graphs for different values of the fluid parameters entering into the control volume numerically discussed and conclude. The study concludes that increasing the Reynolds number results to a reduction in heat and mass transfer and impairs the motion of the nanofluid. An increase in the** Grashof number (Grt), Mass Grashof number (Grc) **results to an increase in the flow velocity which negatively impairs the mixing and heat exchange in the nanofluid thus resulting to a decrease in heat and mass transfer. Increasing the** Magnetic Parameter (M) **leads to an increase in the resistance to the flow of the nanofluid thus reducing the fluid velocity. However, the resistance favors heat and mass transfer as enough time is given for heat exchange and mixing to take place.**

Keywords: **Concentration Boundary Layer, Heat Transfer, Mass Transfer, Magneto-Hydrodynamics (MHD), Nanofluid, Photovoltaic Solar Collector, Thermal Boundary Layer, Velocity Boundary Layer.**

1. INTRODUCTION

1.1 Background Information

Solar energy has a number of advantages over other existing forms of energy such as fossil fuels. For one, it is a clean form of energy as it produces no greenhouse gas emissions that are precursors for environmental degradation and global warming. Solar panels, which are engineering devices used in the collection and conversion of solar radiation are cost effective since they are cheap to buy and require little maintenance and can last for years. This has made it possible for the adoption of the solar energy as a dependable source of energy even in the low economy country such as the third world countries. The efficiency of a solar collector is directly related to the ability of its working fluid to absorb and transfer heat.

However, there are also challenges necessitated by the use of solar power. For instance, the intermittency of sunlight which can limit the ability of the solar system to meet the energy demand during the peak period and the low efficiency of the working fluid have been cited as some of the key challenges. Advances in the energy sector such as the use of nanofluids as the working fluid in the thermal solar collectors are some of the remedies seeking to address existing challenges.

Nanofluids are a new class of heat transfer fluids that is showing promising results for use as a working fluid in solar collectors. [6] Nanofluids are created by dispersing nanometer sized particles in a base fluid typically water or oil. The addiction of this nanoparticles in the base fluid significantly enhances its thermal properties including thermal conductivity, convective heat transfer coefficient and heat capacity. In addition to improving the thermal efficiency of solar collector, nanofluids also helps reduce the size and weight of the solar system. This is because the higher thermal conductivity of the nanofluid allows for compact and efficient heat exchanger to be used which helps reduce the overall size and weight of the collector.

In his study on increasing heat transfer in a flat plate solar collector using various forms of turbulence induced elements on a hybrid nanofluid, Hossein et. al (2022) concluded that an increase in the Reynolds number resulted to a decrease in the heat transfer between the working fluid and the receiver tube thus resulting to a lower temperature output.

Experimental results by Javaniyan et. al (2017) on the thermal entropy generation for a flat plate thermal solar collector filled with porous media concluded that higher values of Reynolds number are more effective in lower reduced temperatures and a lower value of the Reynolds number resulted to a higher heat transfer. The study concluded that an increase in the Reynolds number resulted to an increase in the absorbed het parameter and a decrease in the removed energy parameter. Thus, the collector general efficiency decreased with an increase in the Reynolds number.

Similarly, according to the research undertaken by Selimendigi et. al (2015), on the analysis of the thermal performance of a photovoltaic thermal solar collector with SiO_2 - water nanofluid, the thermal and total efficiency of a flat plate solar collector increases with the addition of nanoparticles volume fraction, a higher value of solar radiation with lower values of convective heat transfer coefficient and inlet temperature for a flat plate solar collector.

A review of the above studies on the heat and mass transfer of MHD nanofluid flow in solar collectors shows that the studies concentrated on flat solar panel collectors with water-based nanofluids and applying steady-state scenarios. The effects of Reynolds number parameter variation on heat and mass transfer for MHD flow under cylindrical coordinates were overlooked. Existing studies did not also consider the application of carbon-based nanoparticles which can have a significant impact on various application due to its higher thermal conductivity. Therefore, this research study seeks to bridge the existing knowledge gap by developing a mathematical model that encompasses the use of a carbon-based nanofluid through a curved solar collector thus making use of the cylindrical coordinates. A curved solar collector is ideal since it increases the surface area for heat absorption and thus more efficient in thermal conductivity than flat panel solar collectors. The above cited literature reviews overlooked

1.2 Definitions of Terms

1.2.1 Concentration Boundary Layer

Concentration refers to the measure at which a substrate dissolves in another substance per unit volume. When a concentration gradient exists between the point of inlet and infinite length along the flow region [at the infinite length in the flow from the inlet] a concentration boundary layer is created.

1.2.2 Heat and Mass Transfer.

Heat and mass transfer are engineering processes by which energy and matter are exchanged between physical systems. Heat transfer is the movement of thermal energy within a system or from one system to another typically from a hotter region to a colder region. Mass transfer is the movement of matter from one system to another or from one region of the system to another due to an existence of a concentration gradient.

1.2.3 Magneto-Hydrodynamics (MHD)

Magneto-hydrodynamics (MHD) is a field of physics and engineering that studies the dynamics of electrically conducting fluids in the presence of magnetic fields. The term "magneto-hydrodynamics" refers to the coupling between the magnetic and hydrodynamic (fluid flow) phenomena in such systems.

Novelty Journals

ISSN 2394-9651

International Journal of Novel Research in Physics Chemistry & Mathematics
Vol. 10, Issue 1, pp: (38-51), Month: January - April 2023, Available at: www.noveltyjournals.com

1.2.4 Concentrated Parabolic Thermal Solar Collector

A solar collector is an engineering device that is used in collecting and converting sunlight into thermal energy. The photovoltaic thermal solar collectors are a form of Concentrated Solar Power (CSP) panels that uses mirrors or lenses to focus the sunrays onto a specific area /tube which heats up the fluid or gas i.e. the working fluid in the tube that drives a turbine thus generating electricity. A parabolic surface is selected to maximize of the surface area for harnessing of the sun rays.

1.2.5 Thermal Boundary Layer

The existence of a temperature different between the solid-fluid interface and that at the free stream results to a formation of a thermal boundary layer. The fluid particle in contact with the solid-fluid flows surface acquire the temperature of the surface. Thermal excitement of the particles results to a random movement of the particles which in turn gives rise to temperature transfer. These thermally exited fluid particles in turn exchanges the acquired thermal energy with adjacent fluid particles. These process continues to adjacent fluid particles leading to formation of a temperature gradient.

1.2.6 Velocity Boundary layer.

As the fluid flows past the surface of the object, the collision of the fluid molecules within the fluid and the molecules touching the flow surface reduces the kinetic energy of the molecules. There is formation of a relatively thin layer of fluid formed near the solid-liquid interface with a rapid change in fluid velocity from zero at the no-slip boundary to the maximum at the free stream. The layer is referred to as the velocity boundary layer and it accounts for the presence of the velocity gradients and shear stress of the momentum equation.

2. MATHEMATICAL FORMULATION

The study considers a two dimensional, unsteady, incompressible boundary layer flow with both heat and mass transfer necessitated by the existence of both temperature and concentration gradient of an electrically conducting carbon nanofluid flow in the receiver tube of a parabolic thermal solar collector. A uniform magnetic field $B_{\circ}$ is applied perpendicularly across the fluid flow which in turn induces a magnetic field b along the radial direction of the flow. The effect of the applied and induced magnetic field is neglected along the $z-direction$ of the flow. Thus, the total magnetic field is given as $B=(b,B_{\circ},0)$.

The parabolic thermal solar collector is designed such that all the radiation from the sun are directed to the focal point where the receiver tube filled with carbon nanofluid lies. The receiver tube contains water with graphene nanoparticles dispersed in it. An axisymmetric cylindrical coordinate (r,z) is chosen thus the tangential flow is neglected. The wall of the receiver tube is kept at a higher temperature T_{wall} compared to the nanofluid flow temperature T_{∞}. The temperature difference is maintained and the nanofluid directly in contact with the flow surface is assumed to adopt the temperature of the flow surface. The tangential velocity component is neglected and thus the axisymmetric velocity vector in cylindrical coordinate is expressed as $U=u(u_r,0,u_z)$.

2.1 Specific Governing Equations.

The flow of MHD nanofluid is theoretically described by the three main governing equations in fluid mechanics which are the continuity, momentum, and energy equations. The governing Navier-Stokes equations are modified based on the assumptions which gives rise to the final partial differential equations in cylindrical coordinates that perfectly suit the fluid flow under review.

2.1.1 Continuity Equation.

This principle is based on the conservation of mass, which states that mass cannot be created or destroyed, only transformed from one form to another. The flow of any fluid is possible only and only if the continuity equation is satisfied. Mathematically, the specific continuity equation in the present study is expressed as:

Novelty Journals

ISSN 2394-9651

International Journal of Novel Research in Physics Chemistry & Mathematics
Vol. 10, Issue 1, pp: (38-51), Month: January - April 2023, Available at: www.noveltyjournals.com

$$\frac{\partial u_r}{\partial r}+\frac{u_r}{r}+\frac{\partial u_z}{\partial z}=0 \tag{1}$$

2.1.2 Momentum Equations.

The momentum equation is derived from Newton's second law of motion, which states that the rate of change of momentum of a body is equal to the resultant force acting on the body and acts in the direction of the force. The momentum equation accounts for all the forces driving the flow. In the present study, the Lorentz force that describes the MHD phenomenon and buoyancy force that accounts for variance in density with temperature and concentration are considered. Mathematically, the specific Momentum equations along the radial and axial direction of the flow in the present study are expressed as:

r -Momentum Equation

$$\rho_{nf}\left[\frac{\partial u_r}{\partial t}+u_r\frac{\partial u_r}{\partial r}+u_z\frac{\partial u_r}{\partial z}\right]=-\frac{\partial P}{\partial r}+\mu_{nf}\left(\frac{\partial^2 u_r}{\partial r^2}+\frac{1}{r}\frac{\partial u_r}{\partial r}+\frac{\partial^2 u_r}{\partial z^2}\right)$$
$$+\rho_{nf}(\beta_T)_{nf}(T-T_\infty)+\rho_{nf}(\beta_C)_{nf}(C-C_\infty)$$
$$-B_o{}^2u_r\sigma_{nf} \tag{2}$$

z - Momentum Equation.

$$\rho_{nf}\left[\frac{\partial u_z}{\partial t}+u_r\frac{\partial u_z}{\partial r}+u_z\frac{\partial u_z}{\partial z}\right]=-\frac{\partial P}{\partial z}+\mu_{nf}\left(\frac{\partial^2 u_z}{\partial r^2}+\frac{1}{r}\frac{\partial u_z}{\partial r}+\frac{\partial^2 u_z}{\partial z^2}\right)+\rho_{nf}(\beta_T)_{nf}(T-T_\infty)$$
$$+\rho_{nf}(\beta_C)_{nf}(C-C_\infty)-\left(B_o{}^2u_z+b^2u_z\right) \tag{3}$$

2.1.3 Energy Equation.

The energy equation is a fundamental principle in fluid mechanics that expresses the conservation of energy for a fluid. It states that the total energy of a fluid in a control volume is equal to the sum of its kinetic energy, potential energy, and internal energy, and that this total energy is conserved over time, assuming no sources or sinks of energy are present within the system. In the present study, thermal radiation and Joules heating were considered as the energy source term. Mathematically, the specific energy equation under review is expressed as:

$$(\rho C_P)_{nf}\left[\frac{\partial T}{\partial t}+u_r\frac{\partial T}{\partial r}+u_z\frac{\partial T}{\partial z}\right]=\kappa_{nf}\left[\frac{\partial^2 T}{\partial r^2}+\frac{1}{r}\frac{\partial T}{\partial r}+\frac{\partial^2 T}{\partial z^2}\right]+\frac{16\sigma^* T_\infty{}^3}{3k*}\frac{\partial^2 T}{\partial r^2}+\sigma_{nf}\left(B_o u_r\right)^2 \tag{4}$$
$$+(\rho Cp)\left[D_B\left(\frac{\partial C}{\partial r}\frac{\partial T}{\partial r}+\frac{\partial C}{\partial z}\frac{\partial T}{\partial z}\right)+\frac{D_T}{T_\infty}\left[\left(\frac{\partial T}{\partial r}\right)^2+\left(\frac{\partial T}{\partial z}\right)^2\right]\right.$$

2.1.4 Species Concentration Equation.

The species concentration equation is a fundamental principle in fluid mechanics that expresses the conservation of mass for different chemical species within a fluid. It states that the mass of each species flowing through any given point in a

fluid system must remain constant over time, assuming no sources or sinks of mass are present within the system. The species concentration equation is used to model and predict the transport and mixing of different chemical species within a fluid. In this study, thermophoresis which is the mass flux generated by the existence of temperature and nanoparticle concentration in the nanofluid is considered as the species source term. Mathematically, the specific species concentration equation under review is expressed as:

$$\frac{\partial C}{\partial t}+u_r\frac{\partial C}{\partial r}+u_z\frac{\partial C}{\partial z}=D_B\left[\frac{\partial^2 C}{\partial r^2}+\frac{1}{r}\frac{\partial C}{\partial r}+\frac{\partial^2 C}{\partial z^2}\right]+\frac{D_T}{T_\infty}\left[\frac{\partial^2 T}{\partial r^2}+\frac{1}{r}\frac{\partial T}{\partial r}+\frac{\partial^2 T}{\partial z^2}\right] \quad (5)$$

2.1.5 Magnetic Induction Equation.

The magnetic induction equation in Magnetohydrodynamics (MHD) flow describes the evolution of the magnetic field in an electrically conducting fluid that is influenced by the motion of the nanofluid and is derived from the principle of conservation of magnetic flux. The magnetic induction equation describes how the magnetic field in a fluid changes over time due to fluid motion and electrical currents. The magnetic induction equation accounts for the induced magnetic field in the present study. Mathematically, the specific magnetic induction equation under review is expressed as:

$$\frac{\partial b}{\partial t}=b\frac{\partial u_r}{\partial z}+D_m\left[\frac{\partial^2 b}{\partial r^2}+\frac{1}{r}\frac{\partial b}{\partial r}+\frac{\partial^2 b}{\partial z^2}\right] \quad (6)$$

2.1.6 Boundary Conditions.

The initial and final systems of equations of the control volume under review are subjected to Dirichlet and Neumann boundary conditions and incorporate the slip boundary conditions.

$$\frac{\partial u_r}{\partial r}=0,\frac{\partial u_z}{\partial r}=0,\frac{\partial \mathrm{T}}{\partial r}=0,\frac{\partial C}{\partial r}=0 \quad \text{At r=0 (centerline)}$$

$$u_r=0,u_z=0,T=T_{wall},C=C_{wall} \quad \text{At r=a (wall)}$$

$$u_r=0,u_z=0,\mathrm{T}=\mathrm{T}_\infty,C=C_\infty \quad \text{At z=0 (inlet)}$$

(7)

$$\frac{\partial u_r}{\partial z}=0,\frac{\partial u_z}{\partial z}=0,\frac{\partial \mathrm{T}}{\partial z}=0,\frac{\partial C}{\partial z}=0 \quad \text{At z=L (outlet)}$$

$$u_r=0,u_z=0,\mathrm{T}=\mathrm{T}_\infty,C=C_\infty \quad \text{At t=0 (initial conditions)}$$

3. NON-DIMENSIONALIZATION OF THE GOVERNING EQUATIONS

The governing partial differential equations 1, 2,3,4,5 and 6 alongside their boundary conditions expressed by equation 7 above are transformed into a system of ordinary differential equations by the use of a system of non-dimensional numbers then solved numerically by employing the finite element method. The in the present study the dimensional variables are represented with the superscript (*) star basing the non-dimensionalization on the scaling variables listed below;

International Journal of Novel Research in Physics Chemistry & Mathematics
Vol. 10, Issue 1, pp: (38-51), Month: January - April 2023, Available at: www.noveltyjournals.com

$$r^* = \frac{r}{L}, z^* = \frac{z}{L}, t^* = \frac{tu_\infty}{L}, b^* = \frac{b}{B_\bullet}, \phi = \frac{C - C_\infty}{C_w - C_\infty}, \theta = \frac{T - T_\infty}{T_w - T_\infty},$$

$$p^* = \frac{p}{\rho u_\infty}, u_r{}^* = \frac{u_r}{u_\infty}, u_z{}^* = \frac{u_z}{u_\infty} \tag{8}$$

Using the non-dimensional numbers expressed by equation (8) above, the dimensionless form of the governing equations 1,2,3,4,5 and 6 reduces to;

$$d_1\left[\frac{\partial u_r{}^*}{\partial t^*} + u_r{}^* \frac{\partial u_r{}^*}{\partial r^*} + u_z{}^* \frac{\partial u_r{}^*}{\partial z^*}\right] = -\frac{dP^*}{dr^*} + \frac{d_4}{\mathrm{Re}}\left(\frac{\partial^2 u_r{}^*}{\partial r^{*2}} + \frac{1}{r^*}\frac{\partial u_r{}^*}{\partial r^*} + \frac{\partial^2 u_r{}^*}{\partial z^{*2}}\right)$$

$$+ d_1 Gr_T \theta + d_1 Gr_C \phi - d_2 M^2 u_r{}^* \tag{9}$$

$$d_1\left[\frac{\partial u_z{}^*}{\partial t^*} + u_z{}^* \frac{\partial u_z{}^*}{\partial z^*}\right] = \frac{d_4}{\mathrm{Re}}\left(\frac{\partial^2 u_z{}^*}{\partial z^{*2}}\right) + d_1 Gr_T \theta + d_1 Gr_C \phi + d_2 M^2 \left(1 - b^{*2}\right) \tag{10}$$

$$d_3\left[\frac{\partial \theta}{\partial t^*} + u_r{}^* \frac{\partial \theta}{\partial r^*} + u_z{}^* \frac{\partial \theta}{\partial z^*}\right] = \frac{d_5}{Pe}\left[\left(\frac{\partial^2 \theta}{\partial r^{*2}} + \frac{1}{r^*}\frac{\partial \theta}{\partial r^*} + \frac{\partial^2 \theta}{\partial z^{*2}}\right)\right] + \frac{Rd}{Pe}\frac{\partial^2 \theta}{\partial r^{*2}} + d_4 u_r{}^{*2} M^2 Ec$$

$$+ d_3 Nb\left(\frac{\partial \phi}{\partial r^*}\frac{\partial \theta}{\partial r^*} + \frac{\partial \phi}{\partial z^*}\frac{\partial \theta}{\partial z^*}\right) + Nt\left(\frac{\partial^2 \theta}{\partial r^{*2}} + \frac{\partial^2 \theta}{\partial z^{*2}}\right) \tag{11}$$

$$\frac{\partial \phi}{\partial t^*} + u_r{}^* \frac{\partial \phi}{\partial r^*} + u_z{}^* \frac{\partial \phi}{\partial z^*} = \frac{1}{Sc} \cdot \frac{1}{\mathrm{Re}}\left[\frac{\partial^2 \phi}{\partial r^{*2}} + \frac{1}{r_r^*}\frac{\partial \phi}{\partial r^*} + \frac{\partial^2 \phi}{\partial z^{*2}}\right] +$$

$$\frac{Nt}{Nb} \cdot \frac{1}{Sc} \cdot \frac{1}{\mathrm{Re}}\left[\frac{\partial^2 \theta}{\partial r^{*2}} + \frac{1}{r^*}\frac{\partial \theta}{\partial r^*} + \frac{\partial^2 \theta}{\partial z^{*2}}\right] \tag{12}$$

$$\frac{\partial b^*}{\partial t^*} = b^* \frac{\partial u_r{}^*}{\partial z^*} + \frac{1}{Rm}\left[\frac{\partial^2 b^*}{\partial r^{*2}} + \frac{1}{r^*}\frac{\partial b^*}{\partial r^*} + \frac{\partial^2 b^*}{\partial z^{*2}}\right] \tag{13}$$

The coefficients d1,d2,d3, d4 and d5 in the expressions of the dimensionless form of the governing equation expressed by equation 9-13 above are used to express the thermo-physical relationship between the nanoparticle, base fluid and the nanofluid and are expressed as shown below;

$$d_1 = \frac{\rho_{nf}}{\rho_f} = \left[(1-\varphi)+\left(\frac{\rho_s}{\rho_f}\right)\right]$$

$$d_2 = \frac{\sigma_{nf}}{\sigma_f} = \left[1+\frac{3(\varphi-1)\varphi}{(\varphi+2)-(\varphi-1)\varphi}\right]$$

$$d_3 = \frac{(\rho Cp)_{nf}}{(\rho Cp)_f} = \left[(\varphi-1)+\varphi\frac{(\rho Cp)_s}{(\rho Cp)_f}\right]$$

$$d_4 = \frac{\mu_{nf}}{\mu_f} = \frac{1}{(1-\varphi)^{2.5}}$$

$$d_5 = \frac{\kappa_{nf}}{\kappa_f} = \left[\frac{\kappa_{nf}+2\kappa_f-2\varphi(\kappa_f-\kappa_{nf})}{\kappa_{nf}+2\kappa_f+2\varphi(\kappa_f-\kappa_{nf})}\right] \quad (14)$$

Similarly, the boundary conditions expressed by equation (7) above is given as;

$$\frac{\partial u_r^*}{\partial r^*}=0, \frac{\partial u_z^*}{\partial r^*}=0, b=B_\circ b^*, \frac{\partial \theta}{\partial r^*}=0, \frac{\partial \phi}{\partial r^*}=0 \quad \text{At } r=0$$

$$u_r^*=0, u_z^*=0, b^*=0, \theta=1, \phi=1 \quad \text{At } r=a$$

$$u_r^*=0, u_z^*=0, b^*=1, \theta=0, \phi=0 \quad \text{At } z=0$$

(15)

$$u_r^*=0, u_z^*=0, b^*=0, \theta=0, \phi=0 \quad \text{At } t=0$$

4. NUMERICAL SOLUTIONS

The numerical solution of the flow equations are generated by employing the Finite Difference Method (FDM). The FDM involves dividing the fluid domain into smaller sub-domains, or elements, and approximating the solution of the Partial Differential Equations (PDEs) that govern fluid flows within each element. The fluid domain is discretized into a grid of points, with each point being assigned a set of variables (e.g., velocity, temperature and concentration etc.) that describe the fluid properties at that point. A computational mesh is used to represent the physical domain of the problem as a collection of discrete points, where the solution variables are defined at each point. The mesh is typically constructed by dividing the physical domain of the problem into a grid of equally spaced points. Computing the first order time derivatives using forward difference approximation whereas, first and second order spatial derivatives by the central difference approximation the stencils for the governing equations are expressed as;

$$d_1 * \left[\left(\frac{U_{i,j}^{k+1} - U_{i,j}^{k}}{\Delta t} \right) + \left(U_{i,j}^{k} \right) * \left(\frac{U_{i+1,j}^{k} - U_{i-1,j}^{k}}{2\Delta r} \right) + \left(V_{i,j}^{k} \right) * \left(\frac{V_{i,j+1}^{k} - V_{i,j-1}^{k}}{2\Delta z} \right) \right]$$

$$= \left(\frac{P_{i+1,j}^{k} - P_{i-1,j}^{k}}{2\Delta r} \right) + \frac{d_4}{\mathrm{Re}} * \left[\left(\frac{U_{i+1,j}^{k} - 2U_{i,j}^{k} + U_{i-1,j}^{k}}{(\Delta r)^2} \right) + \left(\frac{1}{r_{i,j}} \right) * \left(\frac{U_{i+1,j}^{k} - U_{i-1,j}^{k}}{2\Delta r} \right) \right. \tag{16}$$

$$\left. + \left(\frac{V_{i,j+1}^{k} - 2V_{i,j}^{k} + V_{i,j-1}^{k}}{(\Delta z)^2} \right) \right] + d_1 * Gr_T * \theta_{i,j}^{k} + d_1 * Gr_C * \phi_{i,j}^{k} + d_4 * M * M * \left(U_{i,j}^{k} \right)$$

$$d_1 * \left[\left(\frac{V_{i,j}^{k+1} - V_{i,j}^{k}}{\Delta t} \right) + \left(U_z \right) * \left(\frac{V_{i,j+1}^{k} - V_{i,j-1}^{k}}{2\Delta z} \right) \right] = \frac{d_4}{\mathrm{Re}} * \left(\frac{V_{i,j+1}^{k} - 2V_{i,j}^{k} + V_{i,j-1}^{k}}{(\Delta z)^2} \right) + d_1 * Gr_T * \theta$$

$$+ d_1 * Gr_C * \phi_{i,j}^{k} + d_2 * M * M * \left(1 - b_{i,j}^{k} * b_{i,j}^{k} \right) \tag{17}$$

$$d_3 * \left[\frac{\theta_{i,j}^{k+1} - \theta_{i,j}^{k}}{\Delta t} + \left(U_{i,j}^{k} \right) * \left(\frac{\theta_{i+1,j}^{k} - \theta_{i-1,j}^{k}}{2\Delta r} \right) + \left(V_{i,j}^{k} \right) * \left(\frac{\theta_{i,j+1}^{k} - \theta_{i,j-1}^{k}}{2\Delta z} \right) \right]$$

$$= \frac{d_5}{Pe} * \left[\left(\frac{\theta_{i+1,j}^{k} - 2\theta_{i,j}^{k} + \theta_{i-1,j}^{k}}{(\Delta r)^2} \right) + \left(\frac{1}{r_{i,j}^{k}} \right) * \left(\frac{\theta_{i+1,j}^{k} - \theta_{i-1,j}^{k}}{2\Delta r} \right) \right.$$

$$\left. + \left(\frac{\theta_{i,j+1}^{k} - 2\theta_{i,j}^{k} + \theta_{i,j-1}^{k}}{(\Delta z)^2} \right) \right] + \frac{Rd}{Pe} \left[\left(\frac{\theta_{i+1,j}^{k} - 2\theta_{i,j}^{k} + \theta_{i,j-1}^{k}}{(\Delta r)^2} \right) + \right.$$

$$d_4 * \left(U_{i,j}^{k} \right) * M * M * Ec + d_3 * Nb * \left[\left(\frac{\phi_{i+1,j}^{k} - \phi_{i-1,j}^{k}}{2\Delta r} \right) * \left(\frac{\theta_{i+1,j}^{k} - \theta_{i-1,j}^{k}}{2\Delta r} \right) \right.$$

$$\left. + \left(\frac{\phi_{i,j+1}^{k} - \phi_{i,j-1}^{k}}{2\Delta z} \right) * \left(\frac{\theta_{i,j+1}^{k} - \theta_{i,j-1}^{k}}{2\Delta z} \right) \right] + Nt \left[\left(\frac{\theta_{i+1,j}^{k} - 2\theta_{i,j}^{k} + \theta_{i-1,j}^{k}}{(\Delta r)^2} \right) \right. \tag{18}$$

$$\left. \left. + \left(\frac{\theta_{i,j+1}^{k} - 2\theta_{i,j}^{k} + \theta_{i,j-1}^{k}}{(\Delta z)^2} \right) \right] \right]$$

$$\frac{\phi_{i,j}^{k+1}-\phi_{i,j}^{k}}{\Delta t}+\left(U_{i,j}^{k}\right)*\left(\frac{\phi_{i+1,j}^{k}-\phi_{i-1,j}^{k}}{2\Delta r}\right)+\left(V_{i,j}^{k}\right)*\left(\frac{\phi_{i,j+1}^{k}-\phi_{i,j-1}^{k}}{2\Delta z}\right)$$

$$=\frac{1}{Sc}*\frac{1}{\mathrm{Re}}*\left[\left(\frac{\phi_{i+1,j}^{k}-2\phi_{i,j}^{k}+\phi_{i-1,j}^{k}}{(\Delta r)^2}\right)+\left(\frac{1}{r_{i,j}^{k}}\right)*\left(\frac{\phi_{i+1,j}^{k}-\phi_{i-1,j}^{k}}{2\Delta r}\right)\right.$$

$$\left.+\left(\frac{\phi_{i,j+1}^{k}-2\phi_{i,j}^{k}+\phi_{i,j-1}^{k}}{(\Delta z)^2}\right)\right]+\frac{1}{Sc}*\frac{1}{\mathrm{Re}}*\frac{Nt}{Nb}\left[\left(\frac{\phi_{i+1,j}^{k}-2\phi_{i,j}^{k}+\phi_{i-1,j}^{k}}{(\Delta r)^2}\right)+\right.$$

$$\left.\left(\frac{1}{r_{i,j}^{k}}\right)*\left(\frac{\phi_{i+1,j}^{k}-\phi_{i-1,j}^{k}}{2\Delta r}\right)+\left(\frac{\phi_{i,j+1}^{k}-2\phi_{i,j}^{k}+\phi_{i,j-1}^{k}}{(\Delta z)^2}\right)\right] \tag{19}$$

$$\frac{b_{i,j}^{k+1}-b_{i,j}^{k}}{\Delta t}=\left(b_{i,j}^{k}\right)*\left(\frac{b_{i,j+1}^{k}-b_{i,j-1}^{k}}{2\Delta z}\right)+\frac{1}{Rm}*\left[\left(\frac{b_{i+1,j}^{k}-b_{i-1,j}^{k}}{2\Delta r}\right)\right.$$

$$\left.+\left(\frac{1}{r_{i,j}^{k}}\right)*\left(\frac{b_{i+1,j}^{k}-b_{i-1,j}^{k}}{2\Delta r}\right)+\left(\frac{b_{i,j+1}^{k}-2b_{i,j}^{k}+b_{i,j-1}^{k}}{(\Delta z)^2}\right)\right] \tag{20}$$

The resulting systems of ordinary differential equations expressed by equations 16-20 alongside their boundary conditions expressed by equation 15 are simulated using MATLAB to obtain the profiles of the flow variables.

5. RESULTS AND DISCUSSIONS

For various values of the physical parameters involved, numerical computations were performed. These parameters included thermal Grashof number (Grt), Mass Grashof number (Grc), and Magnetic Parameter (M). The accuracy of the numerical method and analysis is checked against the previously published results and an excellent agreement has been obtained in relation to the theoretical and experimental analysis undertaken by Javaniyan et. al (2017), alongside other recent numerical simulation and analysis of MHD flows carried out by key researchers in the cited literature.

Figure 1

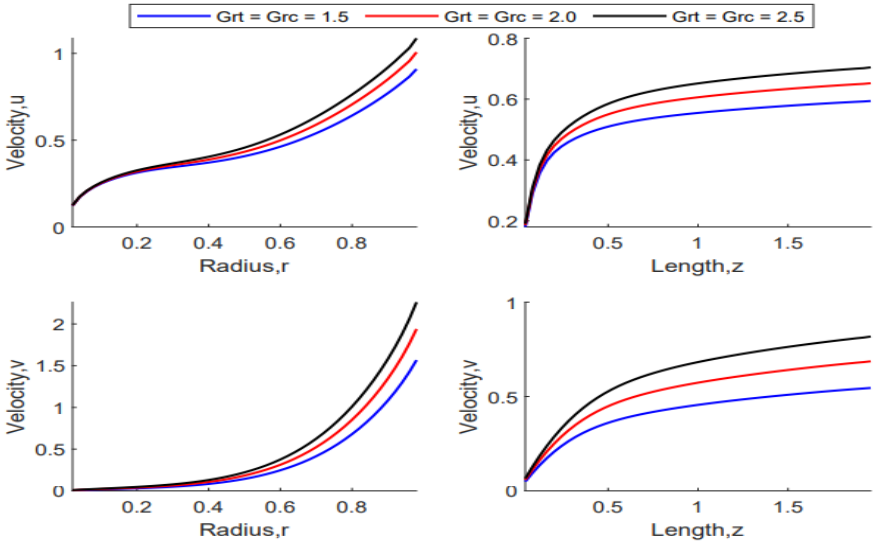

Figure 1 above shows the variations of both the thermal and mass Grashof parameters and its effects on the velocity of a nanofluid flowing past a parabolic surface. The figures depicts that an increase in both the Mass and Thermal Grashof number results to an increase in both the primary and secondary velocities in the r and z direction of the nanofluid flow. The Grashof number is of significance in determining the variation between the buoyancy force and the viscous force restraining the flow of the nanofluid.

Figure 2

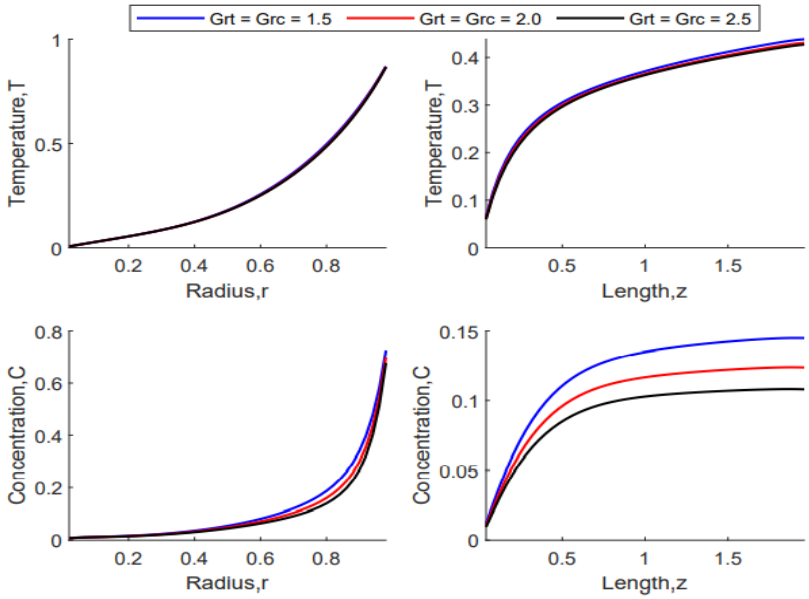

Figure 2 above shows the variations of both the thermal and mass Grashof parameters and its effects on heat and mass transfer of a nanofluid flowing past a parabolic surface. The graphical presentation on temperature variation shows that an increase in the thermal Grashof number results to a decrease in heat transfer of the nanofluid. This is attributed to the increase in the fluid velocity as depicted in **Figure 1** above thus the fluid in contact with the flow surface has minimal time for heat absorption and transfer. The graph on concentration profile also depicts a decrease in the nanofluid concentration

Novelty Journals

ISSN 2394-9651

International Journal of Novel Research in Physics Chemistry & Mathematics
Vol. 10, Issue 1, pp: (38-51), Month: January - April 2023, Available at: www.noveltyjournals.com

with an increase in the mass Grashof number. This is because an increase in the flow velocity impairs the mixing of the nanofluid as it flows down the flow surface.

Figure 3

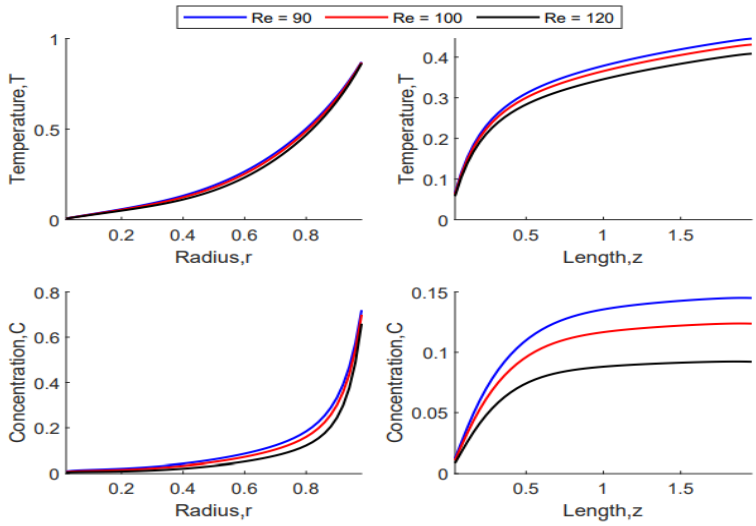

Figure 3 above depicts effects of varying the Reynolds number parameters on temperature and concentration profiles. As shown in the figure, an increase in the Reynolds number leads to a reduction in temperature and concentration both along the r and z direction of the flow. This is consistent with the experimental findings of Ehsan Ebrahimnia-Bajestan et. al. (2016). This is because, an increase in the Reynolds number leads to an increase in the nanofluid flow rate and heat transfer coefficient (Thermal Grashof number), see **Figure 2** above which in turn resuts to a reduction of nanofluid outlet temperature and concentration.

Figure 4

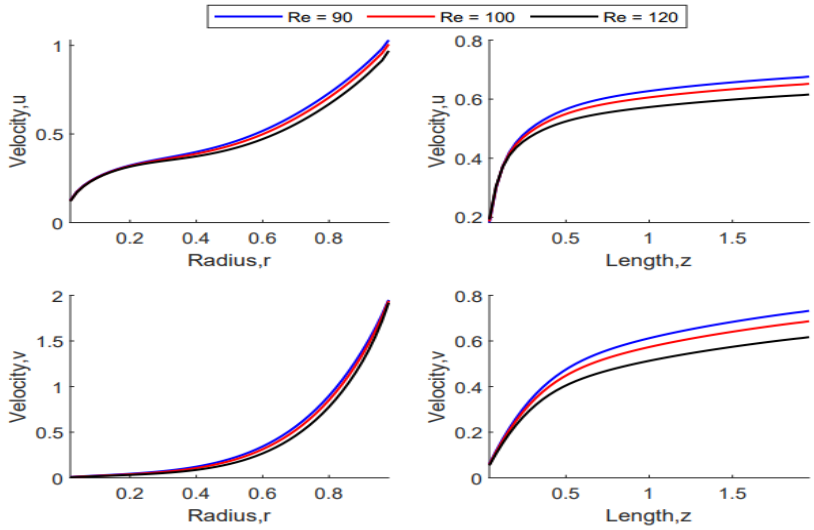

Figure 4 depicts effects of varying the Reynolds number parameters on the velocity profiles. As shown in the figure, an increase in the Reynolds number leads to a reduction in both the primary and secondary velocities along the r and z directions. Since an increase in the Reynolds number leads to a decrease in temperature and concentration and that the motion of the nanofluid is primarily dependent on the temperature and concentration gradient, thus the fluid velocity decreases both in the r and z directions.

Novelty Journals

ISSN 2394-9651

International Journal of Novel Research in Physics Chemistry & Mathematics
Vol. 10, Issue 1, pp: (38-51), Month: January - April 2023, Available at: www.noveltyjournals.com

Figure 5

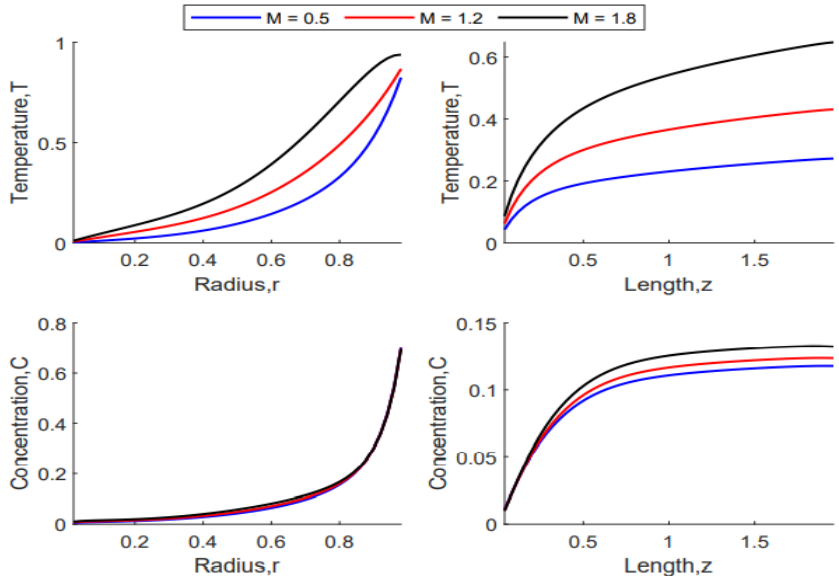

Figure 5 presents the effects of varying the magnetic parameter M on the thermal and concentration profiles. From the figures, it is observed that an increase in the magnetic parameter M favors both heat and mass transfer. The heat transfer increases when M increases. This is due to the production of heat as a result of viscous formation by high resistance of the fluid when there is magnetic field rises. This viscous property produce heat which enhances the temperature distribution. The increase in the magnetic parameter takes effect on the concentration on the nanofluid as the flow nears the boundary at $r = N$. The interference between the fluid magnetic field and the induced magnetic field favors the mixing of the nanoparticles thus boasting the concentration of the nanofluid.

Figure 6

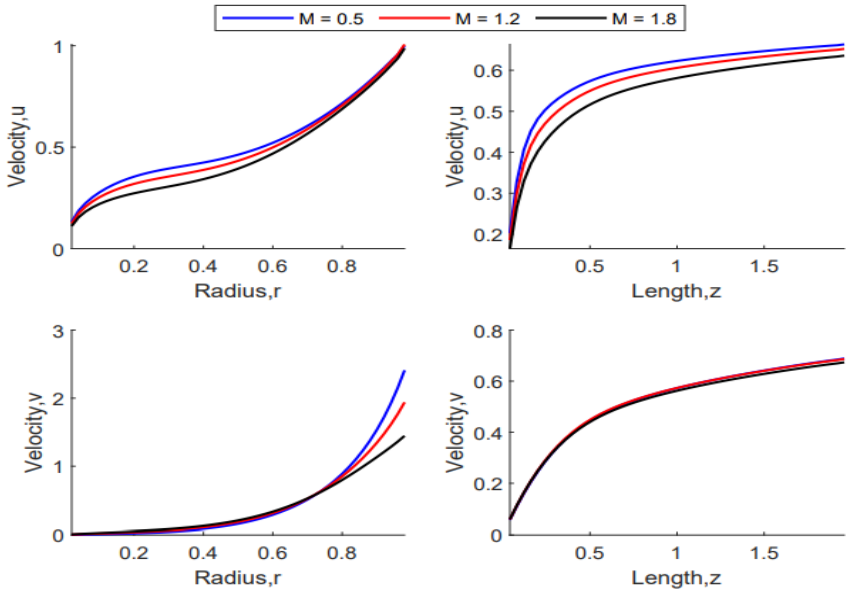

Figure 6 displays the effect of varying the magnetic parameter M on the nanofluid flow velocity. From the figures, it is observed that velocity of the flow decreases significantly throughout the fluid domain with increasing values of magnetic

parameter M . Due to a stronger magnetic field the dimensionless velocity distribution reduces along the flow regime. Application of a magnetic field to an electrically conducting fluid results to formation of Lorentz force which impedes the fluid velocity. The Lorentz force causes a reduction in the fluid velocity within the boundary layer as the magnetic field opposes the transport phenomena.

6. CONCLUSION

The effects of thermal Grashof number (Grt), Mass Grashof number (Grc), and Magnetic Parameter (M) and relevant thermo-physical properties on velocity, temperature, skin friction and local Nusselt number on MHD nanofluid flow are considered in this paper. The present study concludes that:

a) An increase in both the Mass and Thermal Grashof number results to an increase in both the primary and secondary velocities in the r and z direction of the parabolic nanofluid flow. However, an increase in the Mass and Thermal Grashof number results to a decrease in the outlet nanofluid temperature and concentration as an increase in the flow velocity impairs convection heat transfer and nanofluid mixing.

b) An increase in the Reynolds number leads to a reduction in the fluid temperature and concentration both along the r and z direction of the flow. Since an increase in the Reynolds number leads to a decrease in temperature and concentration and that the motion of the nanofluid is primarily dependent on the temperature and concentration gradient, thus the fluid velocity also is impaired.

c) An increase in the magnetic parameter M favors both heat and mass transfer. The heat transfer increases when M increases. This is due to the production of heat as a result of viscous formation by high resistance of the fluid when there is magnetic field rises. This viscous property produce heat which enhances the temperature distribution. The interference between the fluid magnetic field and the induced magnetic field favors the mixing of the nanoparticles thus boasting the concentration of the nanofluid. However, the formation of high resistance to the fluid flow impairs the fluid velocity, thus an increase in the magnetic parameter results to a decrease in the fluid velocity.

d) An induced magnetic field serves as a proper controlling parameter for MHD fluid flow and heat transfer. It also helps maximize the thermodynamic efficiency through altering of the fluid velocity thus maintaining it at optimum ranges for thermal regulation.

ACKNOWLEDGEMENTS

The author expresses his cordial gratitude to Dr. Kimathi and Dr. Muli of the Department of Mathematics of Machakos University, Kenya and the former Director of the Directorate of Criminal Investigations, Kenya Mr. George Kinoti, CBS for their encouragement and support during the undertaking of this research.

REFERENCES

[1] Ehsan Ebrahimnia-Bajestan, F. Y. (2016, July). Investigating the performance of a water-based photovoltaic/thermal (PV/T) collector in laminar and turbulent flow regime. Renewable Energy. doi:10.1016/j.renene.2016.07.004

[2] H. Javaniyan Jouybari, S. S. (2017). Experimental investigation of thermal performance and entropy generation of a flat-plate solar collector that filled with porous media. Elsevier.

[3] Habib-Olah Sayehvand, S. A. (2017, September). MHD Nanofluid flow with viscous dissipation and Joules heating through a permeable channel. Frontier in Heat and Mass Transfer. doi:10.5098/html.9.30

[4] Hossein Nabi, M. P. (2022, May). Increasing heat transfer in flat plate solar collectors using various forms of turbulence-inducing elements and CNTs-CuO hybrid nanofluids. Case Studies in Thermal Engineering, 33. doi:101901

[5] Mahani Ahmed Kardri, N. B. (2021). Magmetohydrodynaic flow past a nonlinear stretching o shrinking cylinder in nanofluid with viscous dssipatonand heat generation effect. Journal of Advanced Research in Fluid Mechanics and Thermal Sciences.

[6] Mohammad Reza Saffarian, M. M. (2020, February). Heat transfer enhancement in a flat plate solar collector with different flow path shapes using nanofluid. Renewable Energy, Volume 146, 2316-2329. doi:https://doi.org/10.1016/j.renene.2019.08.081

[7] Selimefendigil, A. J. (2018, November). Numerical Analysis for Thermal Performance of a Photovoltaic Thermal Solar Collector with SiO - Water Nanofluid. Applied Sciences. doi:10.3390/app8112223

[8] Umar Khan, A. A.-D. (2019). Modified MHD Radiative Mixed Convective Nanofluid Flow Model with Consideration of the Impact of Freezing Temperature and Molecular Diameter. (1. 8. Symmetry 2019, Ed.) Retrieved from https://doi.org/10.3390/sym11060833

[9] Yacine Khetib, A. A. (2022, June). Influence of using innovative turbulators on the exergy and energy efficacy of flat plate solar collector with DWCNTs-TiO2/water nanofluid. Sustainable Energy Technologies and Assessments, 51, 101855. doi:https://doi.org/10.1016/j.seta.2021.101855